Food Packaging and Shelf Life 21 (2019) 100357

Contents lists available at ScienceDirect

Food Packaging and Shelf Life

journal homepage: www.elsevier.com/locate/fpsl

Preparation, characterization and antimicrobial properties of electrospun polylactide films containing *Allium ursinum* L. extract

Tanja Radusin[a,b,*], Sergio Torres-Giner[c], Alena Stupar[a], Ivan Ristic[d], Aleksandra Miletic[d], Aleksandra Novakovic[a], Jose Maria Lagaron[c]

[a] University of Novi Sad, Institute of Food Technology, Bul. Cara Lazara 1, 21000 Novi Sad, Serbia
[b] Nofima - Norwegian Institute of Food, Fisheries and Aquaculture Research, 1430 Ås, Norway
[c] Novel Materials and Nanotechnology Group, Institute of Agrochemistry and Food Technology (IATA), Spanish Council for Scientific Research (CSIC), Calle Catedrático Agustín Escardino Benlloch 7, 46980 Paterna, Spain
[d] University if Novi Sad, Faculty of Technology, Bul. Cara Lazara 1, 21000 Novi Sad, Serbia

ARTICLE INFO

Keywords:
Electrospinning
Natural extracts
Nanoencapsulation
Active food packaging

ABSTRACT

Novel active films of polylactide (PLA) containing extract of *Allium ursinum* L. (AU), also called wild garlic, at 10 wt% were succesfully prepared by the electrospinning technology. Electrospinning of the AU-containing PLA solutions yielded fibers in the 1–2 μm range with a beaded-like morphology, suggesting that the AU extract was mainly encapsulated in certain fiber regions. The resultant electrospun mats were then subjected to annealing at 135 °C to obtain continuous films of application interest in active packaging. The film cross-sections revealed that the AU extract was incorporated into the PLA matrix in the form of micro-sized droplets. The thermal properties showed that the AU extract addition plasticized the PLA matrix and also lowered its crystallinity degree as it disrupted the ordering of the PLA chains by hindering their folding into the crystalline lattice. Thermal stability analysis indicated that the natural extract positively contributed to a delay in thermal degradation of the biopolymer and it was thermally stable when encapsulated in the PLA film. The AU extract incorporation also produced a mechanical reinforcement on the electrospun PLA films and improved slightly the water barrier performance. Finally, a significant antimicrobial activity of the electrospun PLA films containing the natural extract was achieved against foodborne bacteria.

1. Introduction

The food packaging industry presents one of the fastest growing sectors nowadays. New trends in food packaging include food waste reduction, modified atmosphere packaging (MAP), optimization in packaging design, preservation of packaged food products and shelf life extension, active and intelligent packaging, and partial or total substitution of petrochemical sources with renewable ones, among others (Han, 2005; Torres-Giner, Gil, Pascual-Ramírez, & Garde-Belza, 2018). These topics are drivers leading to the development of new food packaging systems that can significantly contribute in ensuring food safety as well as enhancing food science and nutrition. Therefore, in the food packaging area, new approaches go towards the complete or partially substitution of conventional plastics by renewable resources such as biomass. In this sense, polylactide (PLA) is nowadays the most close-to-market biopolymer, having similar physical properties as polyethylene terephthalate (PET) and polystyrene (PS) and with potential applications in various fields such as food packaging, drug delivery systems, biomedical applications, *etc.* (Quiles-Carrillo, Montanes, Sammon, Balart, & Torres-Giner, 2018; Torres-Giner, Gimeno-Alcañiz, Ocio, & Lagaron, 2011).

Additionally, the use of natural antimicrobial compounds in both food and food packaging products has gained a considerable attention by both the consumers and the food industry in order to enhance food quality (Yildirim et al., 2018). The antimicrobial activity against foodborne pathogens of essential oils and natural extracts is well-known for a long time and several research studies have been published on this topic (Benkeblia, 2004). Therefore, both essential oils and natural extracts have been widely applied to improve the antimicrobial and/or antioxidant properties of food packaging materials (López de Dicastillo et al., 2011; López de Dicastillo, Bustos, Guarda, & Galotto, 2016; Suppakul, Miltz, Sonneveld, & Bigger, 2003; Wang & Rhim, 2016). Natural extracts can be easily obtained by extraction methods using various solvents from either fresh plants or milled dried plants. Allium

* Corresponding author at: Nofima-Norwegian Institute of Food, Fisheries and Aquaculture Research, 1430, Ås, Norway.
E-mail address: tanja.radusin@nofima.no (T. Radusin).

https://doi.org/10.1016/j.fpsl.2019.100357
Received 8 February 2019; Received in revised form 29 May 2019; Accepted 27 June 2019
Available online 01 July 2019

species have been widely used in various industrial sectors as both edible and medicinal plants due to their potential health benefits (Sobolewska, Podolak, & Makowska-Was, 2013) and they have also received a special attention for their antimicrobial activity (Ivanova, Mikhova, Najdenski, Tsvetkova, & Kostova, 2009; Kyung, 2012). However, the genuine garlic bulbs may present certain limitations from an application point of view due to their strong and intrinsic unpleasant pungency. As opposite, wild garlic, that is, *Allium ursinum* L. (AU), is recognized for its milder taste and extensive application in food and medicine (Sobolewska et al., 2013). In particular, wild garlic is a rich source of phenolic and sulfur compounds and its extracts have been widely characterized by having high antibacterial and antioxidant activity. As a result, AU extract incorporated into PLA films has recently provided significant antimicrobial activity as well as some improvements in materials properties (Radusin et al., 2019). However, it is currently a challenge to encapsulate AU extract in polymer matrices using conventional melt-processing techniques such as extrusion and injection molding since their active components are thermolabile.

The electrospinning technology offers the option to form high-performance active and bioactive materials composed of polymer yarns of nanofibers with high surface-to-volume ratios at room conditions (Cherpinski et al., 2018; Drosou, Krokida, & Biliaderis, 2017; Torres-Giner, Pérez-Masiá, & Lagaron, 2016). Main principle of electrospinning is based on the application of high electric fields, in the form of high voltages, to viscoelastic polymer-based solutions containing the active or bioactive ingredients (Fernandez, Torres-Giner, & Lagaron, 2009; Torres-Giner, Wilkanowicz, Melendez-Rodriguez, & Lagaron, 2017). The resultant nonwoven mats, based on nanofibers containing the active principles, can be directly applied in the form of coatings or interlayers in films to form novel packaging systems (Torres-Giner, 2011; Torres-Giner, Martinez-Abad, & Lagaron, 2014; Torres-Giner, Busolo, Cherpinski, & Lagaron, 2018). Alternatively, the electrospun mats can be subjected to a thermal post-treatment at a temperature below the biopolymer melting point, the so-called “annealing”, to form continuous transparent films that are more suitable for packaging applications (Cherpinski, Torres-Giner, Cabedo, & Lagaron, 2017). Moreover, since the processing times during annealing are relatively short, in the order of few seconds, the volatile principles contained in the fibers are actively preserved (Figueroa-Lopez, Vicente, Reis, Torres-Giner, & Lagaron, 2019).

The electrospinning technique has recently drawn a great deal of attention for the preparation of different antimicrobial polymer-based systems, especially by the encapsulation and controlled release of natural compounds. For instance, Kriegel, Kit, McClements, and Weiss (2009)) successfully incorporated eugenol, a lipophilic antimicrobial phytophenol that is the predominant constituent of clove (*Syzygiumaromaticum*) EO, into a blend of polyvinyl alcohol (PVOH) and cationic chitosan by emulsion electrospinning. The antimicrobial activity of the fabricated nanofibers was higher against *Salmonella typhimurium* (Gram-negative bacteria, G-) than *Listeria monocytogenes* (Gram-positive bacteria, G+). In addition, the eugenol-loaded nanofibers, with diameters in the 57–126 nm range, presented stronger antimicrobial effect when compared to an equivalent eugenol microemulsion, which was attributed to the faster exhaustion and loss of antimicrobial activity of the free system. More lately, Sun, Zhang, and Li (2011) and Su, Zhang, Wang, and Li (2012) incorporated epigallocatechin gallate (EGCG)–CuII complex and nano-sized of Pu-erh tea powder (NPTP), respectively, into electrospun PVOH nanofibers. The resultant electrospun materials exhibited potent and broad antibacterial activity against, for instance, *Escherichia coli*, rendering encouraging results for novel antibacterial materials. In order to increase the sustained release capacity of the fibers, allyl isothiocyanate (AITC), a naturally occurring compound with bactericidal activity, was encapsulated by electrospinning in soy protein isolate (SPI) and PLA fibers making also use of the β–cyclodextrin (β–CD) inclusion complex (Vega-Lugo & Lim, 2009). The release of the antimicrobial compounds from the electrospun fibers, with diameters ranging from 200 nm to 2 μm, was mainly induced by a phenomenon of moisture sorption. Nevertheless, the use of the resultant antimicrobial nanofibers in more close-to-market active packaging applications is yet to be fully determined based on the activation mechanism and/or kinetics for controlled release. In this sense, zein nanocomposite mats containing thymol essential oil were applied as coatings on PLA films (Torres-Giner et al., 2014). The resultant bi-layer films showed high antimicrobial capacity against *Listeria monocytogenes*, a foodborne bacterium, being then very promising in active packaging applications.

In our preliminary research (Radusin et al., 2019), AU was incorporated into PLA films by the solution casting method. The resultant films showed significant antimicrobial activity as well as some improvements in materials properties, encouraging further research activities on this topic. Since conventional melt-processing routes are not suitable for processing PLA materials loaded with the volatile AU extract, the present research explores, for the first time, the incorporation by electrospinning of the wild garlic extract into PLA films.

2. Materials and methods

2.1. Materials

Semi-crystalline PLA was provided from Shenzhen Esun Industrial Co., Ltd (Shenzhen, China), characterized by a number-average molecular weight (M_n) of 60,520 g/mol, a weight-average molecular weight (M_w) of 160,780 g/mol, and polydispersity index (PDI) of 2.66. Dichloromethane (DCM) and dimethyl formamide (DMF) were both purchased from Sigma-Aldrich S.A. (Madrid, Spain).

Dried plant leaves of wild garlic were donated by Fructus doo (BačkaPalanka, Serbia), a local tea factory. Prior to extraction, the as-received material was grinded to reduce the particle size up to 0.325 mm, as determined using sieve sets (Erweka, Heusenstamm, Germany). The extraction process was carried out using a 20.06 W/L ultrasonic power at 80 °C for 80 min using a 70% ethanol-in-water solution at 70 (vol/vol). The plant material-to-solvent ratio was set at 1:5 (wt/wt). After extraction, the solvent was evaporated using a rotary evaporator at 40 °C (rotavapor R-200, heating Bath B-490, vacuum pump V-700, Büchi, Flawil, Switzerland).

2.2. Preparation of electrospun films

The solutions for electrospinning were prepared in a two-step dissolution process. First, an appropriate amount of AU extract was suspended in DCM and, after that, PLA was added to the solution. The resultant solution was stirred for 24 h at room conditions and, 30 min prior to electrospinning, DMF was added to the solution. The DCM/DMF ratio was 70/30 (vol/vol), the concentration of PLA in the solution was 10 wt%, and the AU concentration was 10 wt% (calculated on PLA weight). A neat PLA solution in DCM/DMF was also prepared in the same conditions as the control sample.

The biopolymer solutions were processed by electrospinning using a Fluidnatek® LE-50 lab line from Bioinicia S.L. (Valencia, Spain), equipped with a variable high-voltage 0–30 kV power supply and with temperature and relative humidity (RH) control system. The process was performed at room conditions, that is, 25 °C and 30% RH, for 1 h. Both PLA and PLA + AU solutions were electrospun with a flow-rate of 2000 μl/h and an applied voltage of 14 kV. The tip-to-collector distance was 15 cm for PLA and 17 cm for PLA + AU solution.

The obtained electrospun mats were, thereafter, subjected to annealing using a hydraulic press 4122-model from Carver, Inc. (Wabash, IN, USA). This was optimally performed at 135 °C, without pressure, for 5 ± 1 s. The resultant films were air-cooled at room temperature.

2.3. Characterization

2.3.1. Film thickness and conditioning

The thickness of the electrospun films was measured using a digital micrometer series S00014, having ± 0.001 mm accuracy, from Mitutoyo Corporation (Kawasaki, Japan). Measurements were performed at three random positions and values were averaged.

2.3.2. Scanning electron microscopy

The morphology of the electrospun PLA fibers and the cross-sections of the annealed films were observed by scanning electron microscopy (SEM) using an S-4800 from Hitachi (Tokyo, Japan). Cryofractures of the films were previously obtained from frozen samples using liquid nitrogen. Prior to examination, all samples were fixed to beveled holders using a conductive double-sided adhesive tape, sputtered with a mixture of gold-palladium under vacuum, and observed using an accelerating voltage of 5 kV. Fiber sizes were determined by means of the Image J software version 1.50E using the SEM micrographs in their original magnification. At least 25 micrographs were used for each measurement.

2.3.3. Surface color

Visual color was measured for all the prepared samples with a Konica Minolta Chroma Meter (Tokyo, Japan). The L^* (lightness), a^* (red-green) and b^* (yellow-blue) parameters were read using a D_{65} light source against the white calibration plate. The color difference between two samples ($\Delta E_{ab}{}^*$) was calculated using the following equation:

$$\Delta E_{ab}{}^* = \sqrt{\Delta L^{*2} + \Delta a^{*2} + \Delta b^{*2}} \quad (1)$$

where ΔL* is the difference in L^* (lightness) between two samples (neat PLA and PLA with AU extract) while, similarly, Δa^* and Δb^* are the differences in the a^* (green/red) and b^* (blue/yellow) coordinates, respectively (Khoddami, Wilkes, & Roberts, 2013). For each film, 5 readings were taken, and the average values were determined. $\Delta E_{ab}{}^*$ below 0.5 indicates an imperceptible difference in color, 0.5–1.5 a slight difference, 1.5–3.0 a noticeable difference, 3.0–6.0 a marked difference, 6.0–12.0 an extremely marked difference, and above 12.0 a color of a different shade (Belović, Mastilović, & Kevrešan, 2014).

2.3.4. Infrared spectroscopy

Fourier transform infrared (FTIR) spectra were collected coupling the attenuated total reflection (ATR) accessory Golden Gate of Specac, Ltd. (Orpington, UK) to a Bruker Tensor 37 FTIR equipment (Rheinstetten, Germany). Single spectra were collected by averaging 20 scans at 4 cm^{-1} resolution of the materials in the wavelength range of 4000–400 cm^{-1}.

2.3.5. Thermal properties

Thermal analysis of the electrospun PLA films was carried out on a DSC 7 analyzer from PerkinElmer, Inc. (Waltham, MA, USA) from room temperature to 200 °C in a nitrogen atmosphere using a refrigerating cooling accessory Intracooler 2 from PerkinElmer, Inc. The scanning rate was set at 10 °C/min and an empty aluminum cup was used as the reference. Calibration was performed using an indium sample. The cold crystallization temperature (T_{cc}), enthalpy of cold crystallization (ΔH_{cc}), melting temperature (T_m), and enthalpy of melting (ΔH_m) were obtained from the heating scan whereas the percentage of crystallinity (X_c) was determined using the following expression:

$$Xc = \left[\frac{\Delta Hm - \Delta Hcc}{\Delta H_m^0 \bullet (1\text{-}w)} \right] \bullet 100 \quad (2)$$

where $\Delta H_m{}^0$ = 93.7 J/g is the enthalpy corresponding to the melting of a 100% crystalline PLA sample (Torres-Giner et al., 2011), while the term 1-*w* represents the biopolymer weight fraction in the film.

Thermal stability of the electrospun films was further investigated by means of thermogravimetric analysis (TGA) using a TG-STDA Mettler Toledo model TGA/SDTA851e/LF/1600. The samples were heated from 50 °C to 900 °C at a heating rate of 10 °C/min under nitrogen flow. The characteristic temperatures $T_{5\%}$ and T_{deg} corresponded, respectively, to the onset decomposition temperature (5% of weight loss) and to the degradation temperature measured at the derivative thermogravimetric (DTG) peak maximum. All the thermal tests were carried out, at least, in triplicate.

2.3.6. Wide angle X-ray scattering

Wide angle X-ray scattering (WAXS) measurements were performed using a Bruker AXS D4 ENDEAVOR diffractometer (Billerica, MA, USA). The samples were scanned, at room temperature, in reflection mode using incident Cu K-alpha radiation (Cu k_α = 1.54 Å), while the generator was set up at 40 kV and 40 mA. The data were collected over a range of scattering angles (2θ) comprised in the of 2–40° range.

2.3.7. Mechanical properties

Mechanical properties of the electrospun PLA films were measured using a Universal testing machine Shimatzu EZ test machine (Kyoto 604-8511, Japan) according to the guidelines of ISO 527-1:2012. Samples were previously shaped into strips with dimensions of 50 × 50 mm^2 and stretched at a cross-head speed of 1 mm/min.

2.3.8. Water vapor permeability

The water vapor permeability (WVP) was determined on the electrospun PLA films using the ASTM 2011 gravimetric method. To this end, 5 mL of distilled water was placed inside a Payne permeability cup (∅ = 3.5 cm) from Elcometer Sprl (Hermalle-sous-Argenteau, Belgium). The films were placed in the cups so that on one side they were exposed to 100% RH, avoiding direct contact with water. The cups containing the films were then secured with silicon rings and stored in a desiccator at 0% RH using dried silica gel at 25 °C. Identical cups with aluminum films were used as control samples to estimate water loss through the sealing. The cups were weighed periodically using an analytical balance of ± 0.0001 g accuracy. Water vapor permeation rate (WVRT), also called water permeance when corrected for permeant partial pressure, was determined from the steady-state permeation slope obtained from the regression analysis of weight loss data per unit area as a function of time, in which the weight loss was calculated as the total cell loss minus the loss through the sealing. Permeability was obtained by correcting the permeance by the average film thicknesses. Measurements were performed in triplicate.

2.3.9. Antimicrobial properties

The antimicrobial properties of the film samples were tested against *E. coli* ATCC11105 and *S. aureus* ATCC 6538p microorganisms. Each bacterial strain was grown aerobically in Nutrient Broth (NB, Becton, Dickinson and Company, Franklin Lakes, NJ, USA) for 18 h at 37 °C. The culture obtained was centrifuged at 7000 rpm for 10 min. The pellet was washed in sterile phosphate buffer solution (PBS) and then resuspended in saline in order to obtain a cell suspension of 10^8 CFU/mL. For further procedures, 96-well microplates were used to each well and 100 µl of 10% AU extract, 100 µl of nutrient broth, and 50 µl of bacterial suspensions were added and incubated at 37 °C for 24 h. In order to count viable bacterial cells, 1.8 mL of PBS was added to the tube, thus obtaining a 10^{-1} dilution, which was then serially diluted and 0.1 mL was plated on Plate Count Agar (PCA). After incubation of the plates at 37 °C for 24 h, the number of colonies, corresponding to the number of viable cells, was counted as colony-forming units (CFU)/mL. The percentage of reduction (R) of viable cells was determined, after averaging the triplicate counts, through the equation:

$$R = (a\text{–}b) \times 100 / a \quad (3)$$

where *a* is the number of viable cells in the control (non- treated cells)

and *b* is the number of viable cells in the specimens containing 10% AU extract.

The antimicrobial activity of the electrospun films was evaluated for the above-described bacterial cultures. To this end, an agar slurry solution was prepared by dissolving 0.3 g agar in 100 mL saline medium. The solution was autoclaved at 121 °C for 30 min, cooled at about 40 °C, and inoculated with 1 mL of the prepared cell suspension. The specimens were pre-wetted with sterile saline, placed into a petri dish, and then 0.25 mL of the inoculated agar slurry solution were pipetted onto the specimen. The cell layer was lower than 1 mm in depth over the entire specimen surface. The slurry solution was allowed to dry and then the petri dishes containing the inoculated specimens were placed on a capped box in which 0.5 mm of distilled water was layered in order to avoid sample drying during incubation. After incubation, performed at room temperature for 24 h, the specimen was placed in a sterile tube with 10 mL of saline and shaken for 3 min to allow the complete release of agar slurry from the sample. Serial dilutions of the solution were performed and plated on Mueller Hinton Agar (HiMedia, India) plates that were incubated for 24 h at 37 °C. Each specimen was processed in triplicate and the antibacterial activity was presented in the form of R values in accordance with Eq. (3).

2.4. Statistical analysis

The color data parameters and antimicrobial activity were evaluated using Statistica v. 10 from StatSoft, Inc. (Tulsa, OK, USA). Fisher's least significant difference (LSD) was used at the 95% confidence level ($p < 0.05$).

3. Results and discussion

3.1. Morphology

The morphology of the electrospun PLA fibers was analyzed by SEM and the images of their mats are included in Fig. 1. In Fig. 1a, it can be observed that the electrospinning of the neat PLA solution yielded bead-free fibers with sizes in the 1–2 μm range. In particular, the mean fiber diameter was 1868 ± 388 nm. A similar morphology of PLA fibers was observed by numerous authors, regardless the Mw of the biopolymer and the solvents used to prepare the solutions (Casasola, Thomas, Trybala, & Georgiadou, 2014; Chen, Lin, Fei, Wang, & Gao, 2010; Yang, Xu, Kotaki, Wang, & Ramakrishna, 2004). In relation to the AU-containing PLA fibers, shown in Fig. 1b, one can observe that these electrospun fibers presented a beaded-like structure with a mean size of 4437 ± 933 nm. This suggests that the wild garlic extract was mainly encapsulated in the beaded regions of the fibers. This phenomenon of forming reservoirs along the fibers with encapsulated extract particles has been previously observed in other studies dealing with electrospinning (Jin et al., 2013; Kayaci, Umu, Tekinay, & Uyar, 2013).

Fig. 2 shows the cross-sections of the PLA materials obtained after annealing. Fig. 2a indicates that the thermal post-treatment produced a continuous PLA structure, resulting in a homogenous film with a mean thickness of 21.7 ± 2.1 μm. This process is known to take place as a result of a process of fibers coalescence (Cherpinski et al., 2017). In the case of the AU-containing PLA sample, shown Fig. 2b, the cross-section was 22.3 ± 2.4 μm but it also revealed the existence of two phases as an "island-and-sea" morphology in which the extract was dispersed in the form of droplets of approximately 2.3 ± 0.5 μm in the PLA matrix. Thus, this morphology supports further the successful encapsulation of the AU extract in PLA as micro-sized droplets.

Fig. 3 presents the visual aspect of the prepared electrospun PLA films. One can observe that both films were fully transparent, though the AU-containing sample also developed an intense yellowish color. The color parameters L*a*b* and the total color change were determined and gathered in Table 1. One can observe that the addition of 10 wt% AU extract in PLA yielded a ΔE_{ab}* value of 7.68, that is, it produced an extremely marked difference in the color change of the film sample. Although this change was evident for all color parameters, the most notorious change was recorded in the yellow-green direction, that is, for the -a* and + b* coordinates.

3.2. Chemical analysis

ATR–FTIR spectroscopy was carried out to confirm the encapsulation of the AU extract in PLA. This technique has been successfully applied to determine the chemical composition of encapsulated bioactive compounds in materials obtained by electrospinning (Torres-Giner et al., 2017). In Fig. 4 one can observe that the FTIR spectrum of the electrospun PLA film presented the characteristic bands for this biopolymer. Briefly, the strongest peak of PLA appeared at 1747 cm^{-1}, being assigned to C═O stretching of the biopolyester. Other strong bands were observed at 1267 cm^{-1} and 1079 cm^{-1}, which have been described to arise from the ester C—O and C—O—C stretching vibrations in electrospun PLA materials (Torres-Giner et al., 2011). Bands in the range 1500–1300 cm^{-1} are habitually ascribed to symmetric and antisymmetric deformational vibrations of C—H in methyl (CH_3) groups, in which the peak centered at 1452 cm^{-1} has been assigned to C—H bends from lactic acid moieties (Braun, Dorgan, & Dec, 2006). The FTIR spectra of the free AU extract showed the main absorption in the 3600–3100 cm^{-1} range, which are typically ascribed to components with O—H and N—H bonds (Torres-Giner et al., 2017). The band at ~1080 cm^{-1} is originated from the sulfate group vibration, that is, ν(S═O), whereas other main absorption bands were observed at ~2980 cm^{-1} for the νs(C—H), at 1635 cm^{-1} for the ν(C═C), and at 1635 cm^{-1} for the δ(C—H) (Ilić et al., 2012). The incorporation of the AU extract into the electrospun PLA film was mainly visible by the intensity increase of the group of bands arising in the 3000–2800 cm^{-1} range, which are characteristic for the C—H assignment of allicin. Although these bands

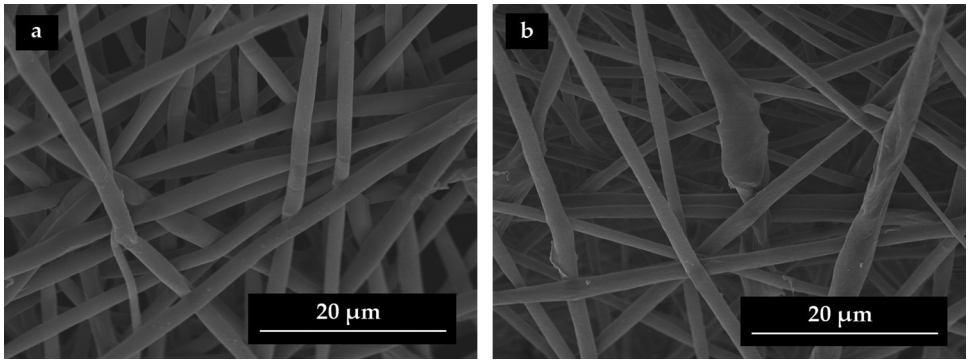

Fig. 1. Scanning electron microscopy (SEM) images of the electrospun fibers of: a) Neat polylactide (PLA); b) PLA containing *Allium ursinum* L. (AU) extract. Scale markers of 20 μm.

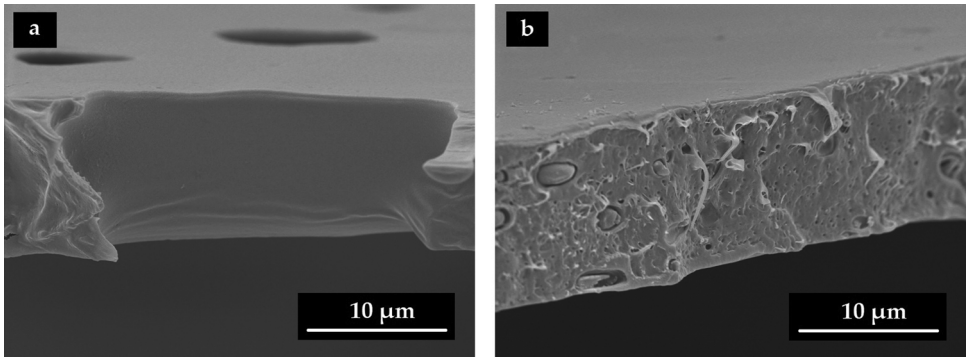

Fig. 2. Scanning electron microscopy (SEM) images of the cross-sections of the electrospun films of: a) Neat polylactide (PLA); b) PLA containing *Allium ursinum* L. (AU) extract. Scale markers of 10 μm.

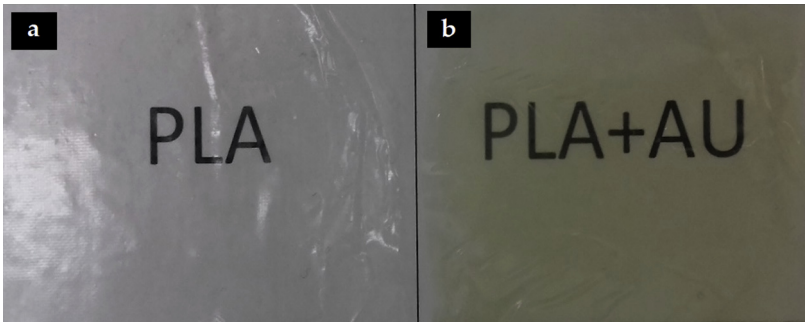

Fig. 3. Contact transparency of the electrospun films of: a) Neat polylactide (PLA); b) PLA containing *Allium ursinum* L. (AU) extract.

Table 1
Color indexes (L*a*b*) of the neat polylactide (PLA) and *Allium ursinum* L. (AU) extract-containing PLA films.

Film sample	L*(D65)	a*(D65)	b*(D65)	ΔE_{ab}
PLA	93.55 ± 0.04 [a]	−0.42 ± 0.01 [a]	4.57 ± 0.015 [a]	–
PLA + AU	91.64 ± 0.02 [b]	−2.32 ± 0.03 [b]	11.75 ± 0.02 [b]	7.68

[a–b]Different letters in the same column indicate a significant difference among the samples ($p < 0.05$).

are also associated to the antisymmetric and symmetric stretching vibrations of CH_2 of polyesters, their intensity was considerably lower in the spectrum of the neat PLA film. This observation would confirm that the extract was successfully incorporated into the electrospun fibers.

3.3. Thermal properties

DSC was employed to characterize the main thermal transitions of the neat PLA and AU-containing PLA films, which are summarized in Table 2. Both films showed similar thermal values, though the incorporation of the AU extract induced some interesting changes in the thermal properties of PLA. The T_g value of PLA was reduced from approximately 48 °C, for the neat PLA film, to 43 °C, for the AU-containing PLA film. This suggests that the presence of the AU extract plasticized the PLA matrix, thus, indicating a good interaction between the natural extract and the PLA chains. However, as seen in previous Fig. 2, a phase separation with no strong interfacial interaction was observed after the AU encapsulation, suggesting that it is possible that some of the AU components were actually dispersed within the biopolymer matrix and interacting with it. Both films presented cold crystallization, with T_{CC} values of approximately 103 °C and 99 °C for the neat PLA film and AU-containing PLA film, respectively. The fact that the cold crystallization process started at lower temperatures for the AU-containing PLA film can be a consequence of the higher mobility of the PLA chains in the presence of AU, but it may also imply that the natural extract can act as nucleating agent for crystal formation. Similar results were reported, for instance, by Llana-Ruiz-Cabello et al. (2015), who observed that the addition of allicin (Proallium®) also decreased PLA's T_g as the active content increased. Moreover, the heating thermograms of the PLA films showed two melting peaks, in the 140–160 °C range, which are linked to classical crystal reorganization upon melting by which imperfect crystals of PLA can order into spherulites with thicker lamellar thicknesses and then melt at higher temperatures (Montava-Jordà, Quiles-Carrillo, Richart, Torres-Giner, & Montanes, 2019). The AU-containing PLA film presented lower T_m values, suggesting that the AU extract also disrupted the ordering of PLA by hindering chain diffusion and folding into the crystalline lattice. This effect was further confirmed by the observed reduction in the X_c values of the PLA films, which decreased from ~13% to 8% after AU incorporation. Therefore, the developed electrospun PLA films were mainly amorphous.

Fig. 5 shows the TGA curves of the neat AU extract and the electrospun PLA and AU-containing PLA films. Thermal stability of the neat natural extract presented a continuous mass loss in a three consecutive degradation steps, being fully degraded at 700 °C. This thermal degradation profile is in agreement with that reported by Tomšik et al. (2019) for wild garlic extract. The first weight loss occurred at approximately 100 °C, of around 2–3%, which can be ascribed to evaporation of solvent, water or some extract volatiles. The second degradation step started at 180 °C, which corresponded to the main mass loss of the natural extract (> 75%), while the last degradation step was seen at around 600 °C for a remaining mass of approximately 20%. This degradation profile confirms that the thermal stability of the AU extract is complex as it occurs over a wide temperature range. As opposite, one can observe that the AU extract was thermally stable when encapsulated in the PLA film since the AU-containing film degraded in a single step. Additionally, the presence of the natural extract slightly increased the thermal stability of PLA. In particular, both the onset degradation temperature, that is, $T_{5\%}$ and T_{deg}, increased after the AU incorporation. In the case of the neat PLA film, the values of $T_{5\%}$ and T_{deg} were 278 °C and 291 °C, respectively, while in the AU-containing

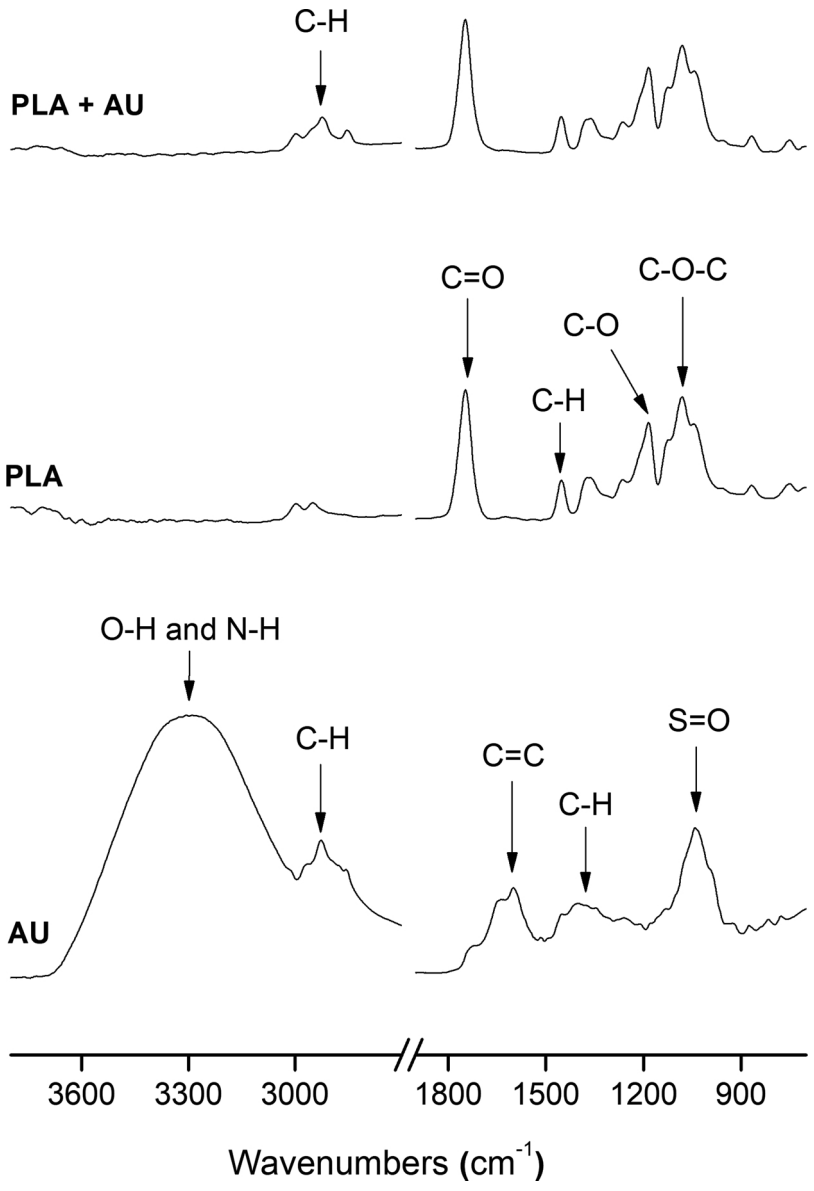

Fig. 4. Fourier transform infrared (FTIR) spectra of, from bottom to top, free *Allium ursinum* L. (AU) extract, electrospun neat polylactide (PLA) film, electrospun AU-containing PLA film.

film these values increased to 302 °C and 304 °C, respectively. This delay in thermal degradation can be ascribed to the potential antioxidant nature of the AU components (Tomšik et al., 2016), resulting in secondary interactions between the extract and the biopolymer. In this regard, extensive H bonding of PLA by polyphenols in the AU has been reported by Zhu et al. (2004). The residual mass at 900 °C was 2.77% and 3.16% for the neat PLA film and the AU-containing PLA film, respectively.

3.4. Crystallinity

WAXS was used to further confirm the presence of AU in the PLA films and also to investigate its influence on the crystalline structure of the biopolymer. The X-ray diffraction profiles of the neat PLA, AU extract, and AU-containing PLA films are shown in Fig. 6. A broad diffraction peak in the 10–25° range was registered for the natural extract. PLA can crystallize in several polymorphic forms (α, β, and γ forms) depending on the preparation conditions (Pilić et al., 2016). However, the WAXD diffractograms of the PLA films indicated that the

Table 2
Thermal properties obtained from the differential scanning calorimetry (DSC) curves in terms of glass transition temperature (T_g), cold crystallization temperature (T_{CC}), melting temperature (T_m), normalized enthalpy of cold crystallization (ΔH_{cc}), normalized enthalpy of melting (ΔH_m), and percentage of crystallinity (X_C) for the neat polylactide (PLA) and *Allium ursinum* L. (AU) extract-containing PLA films.

Film sample	T_g (°C)	ΔH_{CC} (J/g)	T_{CC} (°C)	ΔH_{m1} (J/g)	ΔH_{m2} (J/g)	T_{m1} (°C)	T_{m2} (°C)	X_C (%)
PLA	47.8 ± 0.8	10.26 ± 0.24	102.9 ± 1.0	2.82 ± 0.32	19.84 ± 0.41	147.6 ± 1.5	158.7 ± 0.9	13.2 ± 0.3
PLA + AU	42.7 ± 1.3	21.90 ± 0.36	99.0 ± 0.7	4.31 ± 0.21	24.29 ± 0.18	144.9 ± 2.1	156.9 ± 0.6	7.9 ± 0.2

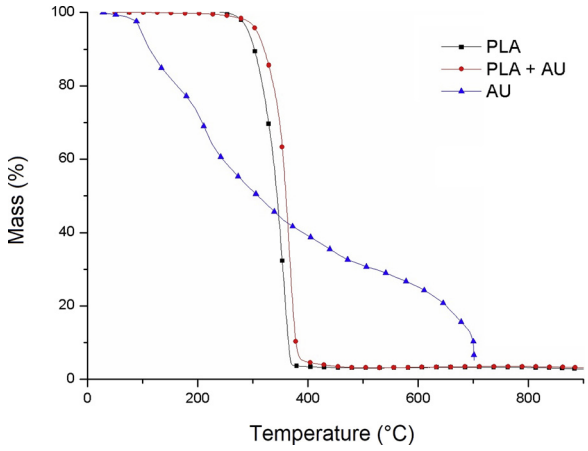

Fig. 5. Thermogravimetric analysis (TGA) curves of free *Allium ursinum* L. (AU) extract and electrospun films of neat polylactide (PLA) and AU-containing PLA.

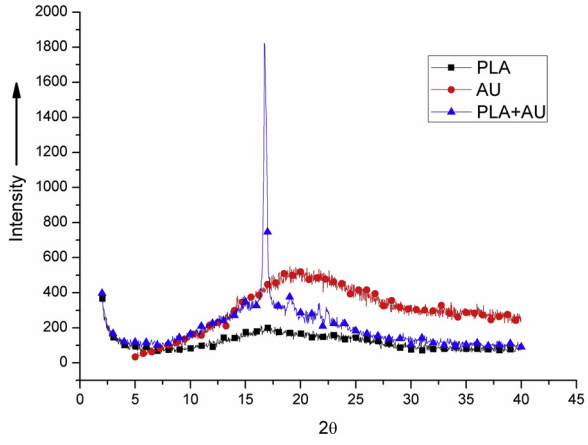

Fig. 6. Wide angle X-ray scattering (WAXS) diffractograms of free *Allium ursinum* L. (AU) extract and electrospun films of neat polylactide (PLA) and AU-containing PLA.

biopolymer samples were relatively amorphous, which is often the case in electrospun fibers and it is also supported by previous DSC analysis. The strong diffraction peak detected at approximately 16.7° after the incorporation of AU into PLA can be ascribed to the presence of the crystalline structures of the natural extract.

3.5. Mechanical properties

Tensile tests were performed on the electrospun films in order to ascertain the effect of the AU incorporation on the mechanical performance of the electrospun PLA films. Fig. 7 shows the stress *versus* strain curves of both PLA film samples, from which the values of tensile strength at yield (σ_y) and elongation at break (ε_b) were obtained. The neat PLA film presented values of σ_y and ε_b of 2.68 ± 0.43 MPa and 4.25 ± 0.83%, respectively. The addition of the wild garlic extract increased the value of σ_y to 4.76 ± 0.58 MPa while ε_b decreased to 3.48 ± 0.67%. Therefore, in spite of the fact that some of the extract components led to a T_g drop and, hence, favored PLA chains mobility, in the overall, the effect of the natural extract on the mechanical performance of the PLA film was that of a reinforcing filler. The ductility impairment attained can be ascribed to the low strong interfacial adhesion between PLA and AU that yielded material discontinuity. Although the here-prepared electrospun PLA films are mechanically softer than equivalent melt-extruded films (Quiles-Carrillo, Montanes, Lagaron, Balart, & Torres-Giner, 2019), they are more flexible and also suitable for packaging applications.

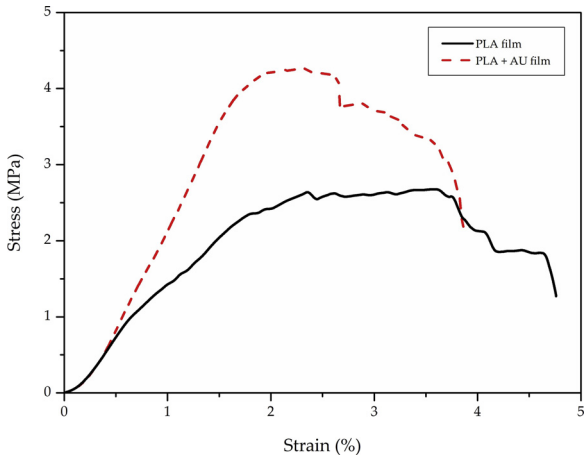

Fig. 7. Typical tensile curves of the electrospun films of neat polylactide (PLA) and *Allium ursinum* L. (AU) extract-containing PLA.

3.6. Barrier properties

The barrier performance is one of the main parameters of application interest for a packaging material, especially for shelf life extension of foodstuff. The WVP of the neat PLA film was 9.21 ± 0.55 × 10^{-14} kg m m^{-2} Pa^{-1} s^{-1}, which is approximately 7.5 times higher than the one recently measured in the same conditions for PLA films prepared by thermo-compression (Quiles-Carrillo et al., 2019). When compared to equivalent films prepared by conventional melt processing methodologies, the reduction observed can be ascribed to the potentially higher degree of porosity produced in some electrospun films due to these materials were formed by a process of fibers coalesce. A similar observation was also recently observed by Cherpinski et al. (2017) for electrospun films made of poly(3-hydroxybutyrate) (PHB). Interestingly, the AU-containing PLA films showed a slightly lower WVP value, that is, 6.86 ± 0.88 × 10^{-14} kg m m^{-2} Pa^{-1} s^{-1}. Since solubility of water vapor in PLA materials is relatively low, indeed water uptake of the biopolymer is below 1 wt% (Quiles-Carrillo, Montanes, Garcia-Garcia et al., 2018), and also the natural extract did not affect the biopolymer crystallinity, one can consider that the AU crystals may impose a more tortuous path for the water molecules to diffuse through. Therefore, the here-developed electrospun films present a medium-to-low barrier to water vapor that is, for instance, only around 3 times less barrier than commercial films made of polyamide 6 (PA6), *i.e.* 2.06 × 10^{-14} kg m m^{-2} Pa^{-1} s^{-1} (Lagaron, 2011).

3.7. Antimicrobial properties

The antimicrobial activity of the free AU extract and the AU-containing PLA film was tested against G- *E. coli* and G + *S. aureus* bacteria. The percentage of reduction of viable cells for each bacterium was calculated referring to the control, that is, a bacterial suspension without antimicrobial agent, and the neat PLA film sample. Results are gathered in Table 3. According to the presented results, the free AU extract was very effective against *E. coli* and showed 100% reduction of viable cells compared to control. Its efficacy against *S. aureus* was also significant, that is, reduction of 53% after 24 h. The here-obtained results are consistent with previous research showing that G- bacteria are more sensitive to garlic extracts than G + ones since the cell wall as well as the cell membrane lipids and polysaccharides may affect the permeability of the *Allium* inhibitory compounds (Perry, Weatherly, Beale, & Randriamahefa, 2009). In relation to the AU-containing PLA film, one can observe that the electrospun film also showed antimicrobial activity against the here-studied microorganisms. The highest antibacterial activity, reported as the R value, of the AU-containing PLA films was observed against *E. coli* (73%), whereas the activity against *S.*

Table 3
Antimicrobial activity of the free *Allium ursinum* L. (AU) extract and the electrospun AU-containing polylactide (PLA) film against *E. coli* and *S. aureus* bacteria.

Bacteria	Sample					
	Positive control*	PLA	AU		PLA + AU	
	Bacterial counts [log (CFU/mL)]	Bacterial counts [log (CFU/mL)]	Bacterial counts [log (CFU/mL)]	Inhibition growth (%)	Bacterial counts [log (CFU/mL)]	Inhibition growth (%)
S. aureus	7.68 ± 0.02 [a]	7.51 ± 0.01[b]	3.51 ± 0.01 [c]	53.0 ± 0.61	5.58 ± 0.03 [d]	27.4 ± 0.57
E. coli	8.05 ± 0.10 [a]	8.02 ± 0.01[a]	N.G.[b]	100.0 ± 0.0	2.16 ± 0.02 [c]	73.0 ± 0.85

Antibacterial activity was quantified as the percentage of growth inhibition of the colony forming units (CFU)/ml. N.G. = No growth was observed.
[a–b]Different letters in the same arrow indicate a significant difference among the samples ($p < 0.05$).
* Bacterial suspensions without added material.

aureus was less pronounced, showing 27.35% reduction of viable cells compared to the neat PLA control. Therefore, AU exhibited total inhibition of *E. coli* and a significant decrease on the growth of *S. aureus*. Accordingly, the incorporation of AU into PLA film resulted in statistically significant decrease ($p < 0.05$) of viable cells compared to the neat PLA control. In particular, it varied from 8.02 log CFU/ml to 2.16 log CFU/ml, for *E. coli*, and from 7.51 log CFU/ml to 5.58 log CFU/ml, for *S. aureus*. The antibacterial activity of the AU-containing PLA films against *E. coli* is of great interest considering that, generally, G- strains are less susceptible to antimicrobial agents (Rios & Recio, 2005). Similar antimicrobial activities were reported against *E. coli* for two concentrations of AU extract (0.5 wt% and 5 wt%) in PLA films prepared by casting (Radusin et al., 2019).

These findings are in agreement with previous reports of packaging films containing 1.2 wt% garlic oil, which were effective to reduce the number of G- and G + bacteria (Gamage, Park, & Kim, 2009). Antimicrobial activity of the genus *Allium* has been mainly attributed to sulfur compounds, mostly allicin and its transformation products (Sobolewska et al., 2013). However, recent studies have shown that other compounds, such as flavonoids, phenols (Cushnie & Lamb, 2005; Daglia, 2011), and saponins (Barile et al., 2007) are also responsible for the observed antimicrobial activity. In this sense, Tomšik et al. (2016), who used the same extraction technique and conditions than the ones described here, obtained a high recovery of polyphenols expressed as a gallic acid equivalent (GAE) in dried plant weight (DW) (1.60 g GAE/100 g) and flavonoids expressed as a catehine equivalent (0.35 g CE/100 g DW). In line with that, the antimicrobial activity of the natural extract is also highly dependent on the preparation and isolation of its active compounds. The type of herbal material, solvent, and extraction technique used to obtain the AU extract play a very important role in the antimicrobial properties. Its antimicrobial activity is mainly assigned to both sulfur and polyphenolic compounds, however, the presence of ferulic and gallic acid are also influential factors (Borges, Ferreira, Saavedra, & Simoes, 2013; Radusin et al., 2019,). Therefore, the here-achieved antimicrobial activity of the wild garlic extract can be a result of a synergistic effect of sulfur and polyphenolic compounds (Cushnie & Lamb, 2005; Pereira et al., 2007; Rauha et al., 2000).

4. Conclusion

Wild garlic extract was incorporated, for the first time, into PLA by electrospinning. This novel technique was effective for the encapsulation of the natural extract whereas the application of a thermal post-treatment at 135 °C generated a continuous and protective film. The encapsulation was observed by SEM and, thereafter, confirmed by chemical analysis using ATR-FTIR spectroscopy. The thermal properties, measured by DSC and TGA, indicated that incorporation of the natural extract resulted in a reduction in T_g and crystallinity degree and it was thermally stable and protected in the biopolymer matrix. WAXS results showed that the PLA films containing AU were mainly amorphous due to the intrinsically low crystallinity of the electrospun materials. The addition of the AU extract slightly reinforced the mechanical strength of the films and it additionally improved the water vapor barrier performance. Finally, the electrospun AU-containing PLA films presented high antibacterial activity against *E. coli* and also a moderate reduction against *S. aureus*. This research result thus confirmed that electrospinning can be regarded as an effective processing technique for the encapsulation and protection of volatile antimicrobial compounds and it can be then used for the preparation of active food packaging films. Therefore, active films achieved through the incorporation of these antimicrobial and sustainable layers or coatings can effectively extend the shelf life and enhance the microbial safety of foodstuff.

Acknowledgments

This paper has been supported by the COST Action FP1405 Active and intelligent fiber-based packaging - innovation and market introduction (ActInPak), FOODStars project Food Product Development Cycle: Frame for stepping Up Research Excellence of FINS (Grant Agreement 692276), the Spanish Ministry of Science, Innovation, and Universities (MICIU, project AGL2015-63855-C2-1-R) and the EU H2020 project YPACK (reference number 773872). Torres-Giner also acknowledges MICIU for his Juan de la Cierva-Incorporación contract (IJCI-2016-29675).

References

Barile, E., Bonanomi, G., Antignani, V., Zolfaghari, B., Sajjadi, S. E., Scala, F., ... Lanzotti, V. (2007). Saponins from Allium minutiflorum with antifungal activity. *Phytochemistry, 68*, 596–603. https://doi.org/10.1016/J.PHYTOCHEM.2006.10.009.

Belović, M. M., Mastilović, J. S., & Kevrešan, Ž. S. (2014). Change of surface colour parameters during storage of paprika (Capsicum annuum L.). *Food and Feed Research, 41*(2), 85–92. Retrieved from http://scindeks-clanci.ceon.rs/data/pdf/2217-5369/2014/2217-53691402085B.pdf.

Benkeblia, N. (2004). Antimicrobial activity of essential oil extracts of various onions (Allium cepa) and garlic (Allium sativum). *LWT - Food Science and Technology, 37*(2), 263–268. https://doi.org/10.1016/j.lwt.2003.09.001.

Borges, A., Ferreira, C., Saavedra, M. J., & Simoes, M. (2013). Antibacterial activity and mode of action of ferulic and gallic acids against pathogenic bacteria. *Microbial Drug Resistance, 19*(4), 256–265. https://doi.org/10.1089/mdr.2012.0244.

Braun, B., Dorgan, J. R., & Dec, S. F. (2006). Infrared spectroscopic determination of lactide concentration in polylactide: An improved methodology. *Macromolecules, 39*(26), 9302–9310. https://doi.org/10.1021/MA061922A.

Casasola, R., Thomas, N. L., Trybala, A., & Georgiadou, S. (2014). Electrospun poly lactic acid (PLA) fibres: Effect of different solvent systems on fibre morphology and diameter. *Polymer, 55*(18), 4728–4737. https://doi.org/10.1016/J.POLYMER.2014.06.032.

Chen, Y., Lin, J., Fei, Y., Wang, H., & Gao, W. (2010). Preparation and characterization of electrospinning PLA/curcumin composite membranes. *Fibers and Polymers, 11*(8), 1128–1131. https://doi.org/10.1007/s12221-010-1128-z.

Cherpinski, A., Torres-Giner, S., Cabedo, L., & Lagaron, J. M. (2017). Post-processing optimization of electrospun submicron poly(3-hydroxybutyrate) fibers to obtain continuous films of interest in food packaging applications. *Food Additives & Contaminants Part A, 34*(10), 1817–1830. https://doi.org/10.1080/19440049.2017.1355115.

Cherpinski, A., Torres-Giner, S., Vartiainen, J., Peresin, M. S., Lahtinen, P., & Lagaron, J. M. (2018). Improving the water resistance of nanocellulose-based films with polyhydroxyalkanoates processed by the electrospinning coating technique. *Cellulose, 25*(2), 1291–1307. https://doi.org/10.1007/s10570-018-1648-z.

Cushnie, T. P. T., & Lamb, A. J. (2005). Antimicrobial activity of flavonoids. *International Journal of Antimicrobial Agents, 26*, 343–356. https://doi.org/10.1016/j.ijantimicag.2005.09.002.

Daglia, M. (2011). Polyphenols as antimicrobial agents. *Current Opinion in Biotechnology, 23*(2), 174–181. https://doi.org/10.1016/j.copbio.2011.08.007.

Drosou, C. G., Krokida, M. K., & Biliaderis, C. G. (2017). Encapsulation of bioactive compounds through electrospinning/electrospraying and spray drying: A comparative assessment of food-related applications. *Drying Technology, 35*(2), 139–162. https://doi.org/10.1080/07373937.2016.1162797.

Fernandez, A., Torres-Giner, S., & Lagaron, J. M. (2009). Novel route to stabilization of bioactive antioxidants by encapsulation in electrospun fibers of zein prolamine. *Food Hydrocolloids, 23*(5), 1427–1432. https://doi.org/10.1016/j.foodhyd.2008.10.011.

Figueroa-Lopez, K. J., Vicente, A. A., Reis, M. A. M., Torres-Giner, S., & Lagaron, J. M. (2019). Antimicrobial and antioxidant performance of various essential oils and natural extracts and their incorporation into biowaste derived poly(3-hydroxybutyrate-co-3-hydroxyvalerate) layers made from electrospun ultrathin fibers. *Nanomaterials, 9*(2), 144. https://doi.org/10.3390/nano9020144.

Gamage, G. R., Park, H. J., & Kim, K. M. (2009). Effectiveness of antimicrobial coated oriented polypropylene/polyethylene films in sprout packaging. *Food Research International, 42*(7), 832–839. https://doi.org/10.1016/J.FOODRES.2009.03.012.

Han, J. H. (2005). *Innovations in food packaging.* Retrieved fromElsevier Academichttps://books.google.rs/books?id=MbVtx091tCUC&dq=Innovations+in+Food+Packaging.+2005,+Elsevier+Ltd.,+London,+UK.&lr=&hl=sr&source=gbs_navlinks_s.

Ilić, D., Ristić, I. S., Nikolić, L., Stanković, M., Nikolić, G., Stanojević, L., ... Nikolić, V. (2012). Characterization and release kinetics of allylthiosufinate and its transformers from Poly(D,L-Lactide) microspheres. *Journal of Polymers and the Environment, 20*(1), 80–87. https://doi.org/10.1007/s10924-011-0337-x.

Ivanova, A., Mikhova, B., Najdenski, H., Tsvetkova, I., & Kostova, I. (2009). Chemical composition and antimicrobial activity of wild garlic Allium ursinum of Bulgarian origin. *Natural Product Communications, 4*(8), 1059–1062.

Jin, G., Prabhakaran, M. P., Kai, D., Annamalai, S. K., Arunachalam, K. D., & Ramakrishna, S. (2013). Tissue engineered plant extracts as nanofibrous wound dressing. *Biomaterials, 34*(3), 724–734. https://doi.org/10.1016/J.BIOMATERIALS.2012.10.026.

Kayaci, F., Umu, O. C., Tekinay, T., & Uyar, T. (2013). Antibacterial electrospun poly (lactic acid) (PLA) nanofibrous webs incorporating triclosan/cyclodextrin inclusion complexes. *Journal of Agricultural and Food Chemistry, 61*(16), 3901–3908. https://doi.org/10.1021/jf400440b.

Khoddami, A., Wilkes, M.a., & Roberts, T. H. (2013). Techniques for analysis of plant phenolic compounds. *Molecules, 18*(2), 2328–2375. https://doi.org/10.3390/molecules18022328.

Kriegel, C., Kit, K. M., McClements, D. J., & Weiss, J. (2009). Nanofibers as carrier systems for antimicrobial microemulsions. Part I: Fabrication and characterization. *Langmuir, 25*(2), 1154–1161. https://doi.org/10.1021/la803058c.

Kyung, K. H. (2012). Antimicrobial properties of allium species. *Current Opinion in Biotechnology, 23*(2), 142–147. https://doi.org/10.1016/j.copbio.2011.08.004.

Lagaron, J. M. (2011). *Multifunctional and nanoreinforced polymers for food packaging.* p. 736Woodhead Publishing Ltd.

Llana-Ruiz-Cabello, M., Pichardo, S., Baños, A., Núñez, C., Bermúdez, J. M. J., Guillamón, E., ... Camean, A. M. (2015). Characterisation and evaluation of PLA films containing an extract of Allium spp. to be used in the packaging of ready-to-eat salads under controlled atmospheres. *LWT - Food Science and Technology, 64*(2), 1354–1361. https://doi.org/10.1016/j.lwt.2015.07.057.

López de Dicastillo, C., Bustos, F., Guarda, A., & Galotto, M. J. (2016). Cross-linked methyl cellulose films with murta fruit extract for antioxidant and antimicrobial active food packaging. *Food Hydrocolloids, 60*, 335–344. https://doi.org/10.1016/j.foodhyd.2016.03.020.

López de Dicastillo, C., Nerín, C., Alfaro, P., Catalá, R., Gavara, R., & Hernández-Muñoz, P. (2011). Development of new antioxidant active packaging films based on ethylene vinyl alcohol copolymer (EVOH) and green tea extract. *Journal of Agricultural and Food Chemistry, 59*(14), 7832–7840. https://doi.org/10.1021/jf201246g.

Montava-Jordà, S., Quiles-Carrillo, L., Richart, N., Torres-Giner, S., & Montanes, N. (2019). Enhanced interfacial adhesion of polylactide/poly(ε-caprolactone)/walnut shell flour composites by reactive extrusion with maleinized linseed oil. *Polymers, 11*(5), 758. https://doi.org/10.3390/polym11050758.

Pilić,.

Pereira, A. P., Ferreira, I. C., Marcelino, F., Valentão, P., Andrade, P. B., Seabra, R., ... Pereira, J. A. (2007). Phenolic compounds and antimicrobial activity of olive (Olea europaea L. Cv. Cobrançosa) leaves. *Molecules, 12*(5), 1153–1162. https://doi.org/10.3390/12051153.

Perry, C. C., Weatherly, M., Beale, T., & Randriamahefa, A. (2009). Atomic force microscopy study of the antimicrobial activity of aqueous garlic *versus* ampicillin against *Escherichia coli* and *Staphylococcus aureus*. *Journal of the Science of Food and Agriculture, 89*(6), 958–964. https://doi.org/10.1002/jsfa.3538.

Quiles-Carrillo, L., Montanes, N., Garcia-Garcia, D., Carbonell-Verdu, A., Balart, R., & Torres-Giner, S. (2018). Effect of different compatibilizers on injection-molded green composite pieces based on polylactide filled with almond shell flour. *Composites Part B Engineering, 147*, 76–85. https://doi.org/10.1016/J.COMPOSITESB.2018.04.017.

Quiles-Carrillo, L., Montanes, N., Sammon, C., Balart, R., & Torres-Giner, S. (2018). Compatibilization of highly sustainable polylactide/almond shell flour composites by reactive extrusion with maleinized linseed oil. *Industrial Crops and Products, 111*, 878–888. https://doi.org/10.1016/J.INDCROP.2017.10.062.

Quiles-Carrillo, L., Montanes, N., Lagaron, J. M., Balart, R., & Torres-Giner, S. (2019). In situ compatibilization of biopolymer ternary blends by reactive extrusion with low-functionality epoxy-based styrene–acrylic oligomer. *Journal of Polymers and the Environment, 27*(1), 84–96. https://doi.org/10.1007/s10924-018-1324-2.

Radusin, T., Tomšik, A., Šarić, L., Ristić, I., Giacinti Baschetti, M., Minelli, M., ... Novaković, A. (2019). Hybrid Pla/wild garlic antimicrobial composite films for food packaging application. *Polymer Composites*. https://doi.org/10.1002/pc.24755.

Rauha, U.-P., Remes, S., Heinonen, M., Hopia, A., Kahkonen, M., Kujala, T., ... Vuorela, P. (2000). Antimicrobial effects of Finnish plant extracts containing flavonoids and other phenolic compounds. *International Journal of Food Microbiology, 56*, 3–12. Retrieved from www.elsevier.nl.

Rios, J. L., & Recio, M. C. (2005). Medicinal plants and antimicrobial activity. *Journal of Ethnopharmacology, 100*(1-2), 80–84.

Sobolewska, D., Podolak, I., & Makowska-Was, J. (2013). Allium ursinum: Botanical, phytochemical and pharmacological overview. *Phytochemistry Reviews, 4*(1), 81–97. https://doi.org/10.1007/s11101-013-9334-0.

Su, Y., Zhang, C., Wang, Y., & Li, P. (2012). Antibacterial property and mechanism of a novel Pu-erh tea nanofibrous membrane. *Applied Microbiology and Biotechnology, 93*(4), 1663–1671. https://doi.org/10.1007/s00253-011-3501-2.

Sun, L., Zhang, C., & Li, P. (2011). Characterization, antimicrobial activity, and mechanism of a high-performance (−)-Epigallocatechin-3-gallate (EGCG)−Cu ^{II} /Polyvinyl alcohol (PVA) nanofibrous membrane. *Journal of Agricultural and Food Chemistry, 59*(9), 5087–5092. https://doi.org/10.1021/jf200580t.

Suppakul, P., Miltz, J., Sonneveld, K., & Bigger, S. W. (2003). Antimicrobial properties of basil and its possible application in food packaging. *Journal of Agricultural and Food Chemistry, 51*(11), 3197–3207. https://doi.org/10.1021/jf021038t.

Tomšik, A., Pavlić, B., Vladić, J., Ramić, M., Brindza, J., & Vidović, S. (2016). Optimization of ultrasound-assisted extraction of bioactive compounds from wild garlic (Allium ursinum L.). *Ultrasonics Sonochemistry, 29*, 502–511. https://doi.org/10.1016/j.ultsonch.2015.11.005.

Tomšik, A., Šarić, L., Bertoni, S., Protti, M., Albertini, B., Mercolini, L., ... Passerini, N. (2019). Encapsulations of wild garlic (Allium ursinum L.) extract using spray congealing technology. *Food Research International, 119*, 941–950. https://doi.org/10.1016/j.foodres.2018.10.081.

Torres-Giner, S., Gil, L., Pascual-Ramírez, L., & Garde-Belza, J. (2018). Packaging: Food waste reduction. In M. Mishra (Vol. Ed.), *Encyclopedia of polymer application: Volume 3*, (pp. 1990–2009). Boca Raton, FL, USA: CRC Press 2018.

Torres-Giner, S., Gimeno-Alcañiz, J. V., Ocio, M. J., & Lagaron, J. M. (2011). Optimization of electrospun polylactide-based ultrathin fibers for osteoconductive bone scaffolds. *Journal of Applied Polymer Science, 122*(2), 914–925. https://doi.org/10.1002/app.34208.

Torres-Giner, S., Busolo, M., Cherpinski, A., & Lagaron, J. M. (2018). Electrospinning in the packaging industry. In E. Kny, K. Ghosal, & S. Thomas (Eds.). *Electrospinning: From basic research to commercialization* (pp. 238–260). .

Torres-Giner, S., Pérez-Masiá, R., & Lagaron, J. M. (2016). A review on electrospun polymer nanostructures as advanced bioactive platforms. *Polymer Engineering and Science, 56*(5), 500–527. https://doi.org/10.1002/pen.24274.

Torres-Giner, S. (2011). *Novel antimicrobials obtained by electrospinning methods. Antimicrobial polymers*. Hoboken, NJ, USA: John Wiley & Sons, Inc261–285. https://doi.org/10.1002/9781118150887.ch10.

Torres-Giner, S., Martinez-Abad, A., & Lagaron, J. M. (2014). Zein-based ultrathin fibers containing ceramic nanofillers obtained by electrospinning. II. Mechanical properties, gas barrier, and sustained release capacity of biocide thymol in multilayer polylactide films. *Journal of Applied Polymer Science, 131*(18), 1–7. https://doi.org/10.1002/app.40768.

Torres-Giner, S., Wilkanowicz, S., Melendez-Rodriguez, B., & Lagaron, J. M. (2017). Nanoencapsulation of Aloe vera in synthetic and naturally occurring polymers by electrohydrodynamic processing of interest in food technology and bioactive packaging. *Journal of Agricultural and Food Chemistry, 65*(22), 4439–4448. https://doi.org/10.1021/acs.jafc.7b01393.

Vega-Lugo, A.-C., & Lim, L.-T. (2009). Controlled release of allyl isothiocyanate using soy protein and poly(lactic acid) electrospun fibers. *Food Research International, 42*(8), 933–940. https://doi.org/10.1016/j.foodres.2009.05.005.

Wang, L.-F., & Rhim, J.-W. (2016). Grapefruit seed extract incorporated antimicrobial LDPE and PLA films: Effect of type of polymer matrix. *LWT - Food Science and Technology, 74*, 338–345. https://doi.org/10.1016/j.lwt.2016.07.066.

Yang, F., Xu, C. Y., Kotaki, M., Wang, S., & Ramakrishna, S. (2004). Characterization of neural stem cells on electrospun poly(L-lactic acid) nanofibrous scaffold. *Journal of Biomaterials Science Polymer Edition, 15*(12), 1483–1497. https://doi.org/10.1163/1568562042459733.

Yildirim, S., Röcker, B., Pettersen, M. K., Nilsen-Nygaard, J., Ayhan, Z., Rutkaite, R., ... Coma, V. (2018). Active packaging applications for food. *Comprehensive Reviews in Food Science and Food Safety, 17*(1), 165–199. https://doi.org/10.1111/1541-4337.12322.

Zhu, B., Li, J., He, Y., Yamane, H., Kimura, Y., Nishida, H., ... Inoue, Y. (2004). Effect of steric hindrance on hydrogen-bonding interaction between polyesters and natural polyphenol catechin. *Journal of Applied Polymer Science, 91*(6), 3565–3573. https://doi.org/10.1002/app.13581.